Oxidized Lipoproteins Promote Resistance to Cancer Immunotherapy Independent of Patient Obesity

Niloufar Khojandi[1], Lindsey M. Kuehm[1], Alexander Piening[1], Maureen J. Donlin[2], Eddy C. Hsueh[3], Theresa L. Schwartz[3], Kaitlin Farrell[3], John M. Richart[4], Elizabeth Geerling[1], Amelia K. Pinto[1], Sarah L. George[5], Carolyn J. Albert[2], David A. Ford[2], Xiufen Chen[6], Justin Kline[6], and Ryan M. Teague[1,7]

ABSTRACT

Antitumor immunity is impaired in obese mice. Mechanistic insight into this observation remains sparse and whether it is recapitulated in patients with cancer is unclear because clinical studies have produced conflicting and controversial findings. We addressed this by analyzing data from patients with a diverse array of cancer types. We found that survival after immunotherapy was not accurately predicted by body mass index or serum leptin concentrations. However, oxidized low-density lipoprotein (ox-LDL) in serum was identified as a suppressor of T-cell function and a driver of tumor cytoprotection mediated by heme oxygenase-1 (HO-1). Analysis of a human melanoma gene expression database showed a clear association between higher *HMOX1* (HO-1) expression and reduced progression-free survival. Our *in vivo* experiments using mouse models of both melanoma and breast cancer revealed HO-1 as a mechanism of resistance to anti-PD1 immunotherapy but also exposed HO-1 as a vulnerability that could be exploited therapeutically using a small-molecule inhibitor. In conclusion, our clinical data have implicated serum ox-LDL as a mediator of therapeutic resistance in patients with cancer, operating as a double-edged sword that both suppressed T-cell immunity and simultaneously induced HO-1–mediated tumor cell protection. Our studies also highlight the therapeutic potential of targeting HO-1 during immunotherapy, encouraging further translational development of this combination approach.

See article by Kuehm et al., p. 227

Introduction

Checkpoint blockade immunotherapy is a well-established cancer treatment, but not all patients achieve a durable response (1, 2). As a result, the goals for human immunotherapy studies have shifted away from just demonstrating clinical efficacy toward improving outcomes for a much broader range of patients with diverse cancer types. This requires new insight into the variables that dictate therapeutic success and failure. More than a third of Americans are considered obese (3), and because obesity is associated with compromised immunity (4), it was initially predicted that patients with cancer who are obese would experience worse outcomes compared with patients who are leaner. Indeed, for breast cancer, obesity is associated with larger tumors that are refractory to anti-VEGF therapy (5). For patients with bladder cancer treated with Bacillus Calmette-Guerin, progression-free survival (PFS) is reduced in overweight and obese patient cohorts (6). Likewise, in a large retrospective analysis of 1,186 patients with melanoma, those with higher body mass index (BMI) experienced shorter survival even when adjusted for age, sex, and stage of disease (7).

These studies support a link between obesity and poor outcomes, but other clinical studies focusing on checkpoint blockade immunotherapy have produced conflicting results. For example, a retrospective analysis of 2,046 patients with melanoma concluded that survival after immunotherapy was either unaffected or even improved in those with higher BMI (8). Interestingly, the impact of obesity on these patients varied slightly between sexes, as male patients who were obese responded better than males who were not obese, whereas the survival of female patients was independent of BMI. In addition, in a cohort of 250 patients with various cancers receiving either anti-PD1 or anti-PDL1, higher BMI correlated with improved survival over a 2-year period, and this was independent of sex (9). This was attributed to a previously undescribed mechanism observed in obese mice whereby higher levels of serum leptin induced PD1 expression on T cells, making them more responsive to PD1 blockade (9, 10). Although this mechanistic link was not confirmed in human patients with cancer, it was supported by correlative expression data in healthy volunteers. Regardless, patient survival data in these latter two studies support the controversial "obesity paradox," where the effect of obesity, which was expected to be overwhelmingly negative, turned out to be neutral or even positive. This paradox has been observed in diverse clinical trials from cancer to cardiovascular disease but the existence of the obesity paradox is now being debated, with some suggesting that adherence to the standard BMI scale (often the only indicator of obesity available in retrospective analyses) masks the truly complicated nature of obesity and metabolic health, thereby skewing interpretation of clinical results (11, 12).

Here, we report a retrospective analysis of 278 patients with cancer who were treated with checkpoint blockade immunotherapies

[1]Department of Molecular Microbiology and Immunology, Saint Louis University School of Medicine, St. Louis, Missouri. [2]Department of Biochemistry and Molecular Biology, Saint Louis University School of Medicine, St. Louis, Missouri. [3]Department of Surgery, Saint Louis University School of Medicine, St. Louis, Missouri. [4]Department of Internal Medicine, Division of Hematology and Oncology, Saint Louis University School of Medicine, St. Louis, Missouri. [5]Department of Internal Medicine, Division of Infectious Diseases, Allergy and Immunology, Saint Louis University School of Medicine, St. Louis, Missouri. [6]Department of Medicine, University of Chicago, Chicago, Illinois. [7]Alvin J. Siteman National Cancer Institute Comprehensive Cancer Center, St. Louis, Missouri.

Note: Supplementary data for this article are available at Cancer Immunology Research Online (http://cancerimmunolres.aacrjournals.org/).

Corresponding Author: Ryan M. Teague, Saint Louis University School of Medicine, 1100 South Grand Boulevard, DRC Room 705, St. Louis, MO 63104. Phone: 314-977-8871; E-mail: ryan.teague@health.slu.edu

Cancer Immunol Res 2021;9:214–26

doi: 10.1158/2326-6066.CIR-20-0358

targeting either PD1, PDL1, or CTLA4. There was no overall consensus among these patients, as BMI alone did not consistently predict survival outcomes. Analysis of freshly isolated peripheral immune cells and tumor-infiltrating lymphocytes (TIL) from patients with melanoma and breast cancer also showed no relationship between immune cell function and BMI. Although higher leptin levels in the plasma of obese patients was observed, there was no evidence linking PD1 expression to either leptin or BMI. This observation has important clinical implications and implies that the paradigm between obesity, leptin, and PD1 may not be universal.

To explore alternative explanations for the range of clinical outcomes observed in patients receiving checkpoint blockade immunotherapy, we performed lipidomic assessments on plasma from patients with melanoma or breast cancer. These studies uncovered a mechanism of treatment resistance whereby high serum cholesterol and oxidized lipoproteins impaired cellular immunity and protected tumors from apoptosis. Obesity is associated with oxidative stress, resulting in dysregulated lipid metabolism such as increased oxidation of serum lipids and cholesterol-rich low-density lipoproteins (LDL; ref. 13). Our clinical data showed higher levels of cholesterol and LDL were associated with decreased survival of patients treated with anti-PD1/L1. Oxidized LDL (ox-LDL) was associated with impaired T-cell immune responses and also the induction of a cytoprotective stress response in human melanoma tumor cells via increased expression of heme oxygenase-1 (HO-1). In mouse models of melanoma and breast cancer, HO-1 cytoprotection shielded melanoma cells from apoptosis and provided resistance to PD1 checkpoint blockade immunotherapy. These *in vivo* studies revealed HO-1 as a molecular target that could be exploited for improved checkpoint blockade immunotherapy outcomes.

Together, our data demonstrate that patient BMI alone is a poor indicator of human tumor immunity and is not predictive of patient survival following checkpoint blockade immunotherapy. Rather, our results point toward a more complex relationship between obesity, diet, and serum lipid accumulation that impairs T-cell immunity and simultaneously promotes tumor cell resistance mechanisms that hinder the success of cancer immunotherapy.

Materials and Methods

Human subjects

Access to data from clinical trial NCT00094653 was obtained through the Bristol-Myers Squibb data-sharing program (https://www.bms.com/researchers-and-partners/clinical-trials-and-research.html). Human blood and tumor tissue samples were obtained from 27 patients with melanoma and 11 patients with breast cancer who received standard-of-care treatment at Saint Louis University Hospital (St. Louis, MO) and provided written informed consent in accordance with the Declaration of Helsinki. Blood from healthy volunteers was collected and analyzed by the Pinto and George labs at Saint Louis University (St. Louis, MO). This analysis was conducted with approval from the Saint Louis University institutional review board (IRB). Data from 30 patients with non-Hodgkin lymphoma treated at the University of Chicago (Chicago, IL) was obtained from Justin Kline following analysis in his laboratory with approval from the University of Chicago IRB. The Gene Expression Profiling Interactive Analysis (GEPIA) database (gepia.cancer-pku.cn) was used to correlate *HMOX1* gene experssion in human melanoma tumors with disease-free survival, independent of treatment. All available 458 anonymous patients with melanoma were stratified by *HMOX1* expression with a median group cutoff of 50% (229 high and 229 low). Patients with melanoma were also stratified by pathologic disease stage (0–IV) with relative *HMOX1* gene expression determined at each stage.

Blood and tissue processing

Whole blood was collected in a Beckton Dickinson Vacutainer with 158 USP units sodium heparin (BD Biosciences, catalog no. 36784). Blood was centrifuged at 1,500 × *g* for 10 minutes at 4°C to separate cells from plasma. Plasma was collected and stored at −80°C. The cellular fraction was resuspended in PBS at three times the original blood volume and overlaid onto Ficoll-Paque PLUS (GE Healthcare Life Sciences, catalog no. 71101900-EH). Peripheral blood mononuclear cells (PBMC) were separated from red blood cells by centrifugation at 2,000 RPM for 30 minutes at 4°C. The PBMC fraction was removed, washed two times in PBS (Invitrogen, catalog no. AM9625), and cryopreserved in 10% DMSO (Thermo Fisher Scientific, catalog no. BP231-1), 40% FBS (Corning, catalog no. 35-011-CV) in RPMI1640 media (Sigma, catalog no. R8758-1L), frozen gradually to −80°C and then stored in liquid nitrogen prior to analysis. Tumor tissue was minced into approximately 2 mm pieces in a 6-well tissue culture plate and digested in collagenase (1 mg/mL in water) and DNAse (0.25 mg/mL in water) for 30 minutes at 37°C. Collagenase (catalog no. C6079) and DNAse (catalog no. DN95) were purchased from Sigma. Tissue pieces were then crushed with a sterile syringe plunger and cells passed through a 40 μM nylon cell strainer (Corning, catalog no. 43750). Cells washed twice in PBS and cryopreserved as described above.

Lipid and leptin quantification

Lipids were extracted from 100 μL of serum using a modified Bligh–Dyer lipid extraction protocol in the presence of heptadecanoyl cholesteryl ester (CE) internal standard, as described previously (14). Lipid extracts were diluted in methanol/chloroform (1/2, vol/vol) and CE species were quantified using electrospray ionization mass spectrometry on a triple quadrupole instrument (Themo Fisher Quantum Ultra) employing shotgun lipidomics (15). CE molecular species were quantified as sodiated adducts in the positive ion mode using neutral loss scanning of 368.5 amu as described previously (16). Total CE concentration was determined by summing up the CE species which were predominantly comprised of linoleoyl and arachidonyl CE. ox-LDL in patient plasma was measured by sandwich ELISA (Mercodia AB; catalog no. 10-1143-01) targeting a conformational epitope that distinguishes it from LDL using a mAb (4E6; ref. 13). Human leptin was measured using an ELISA kit from Crystal Chem (catalog no. 80968) according to the manufacturer's protocol. Total cholesterol, triglycerides, and high-density lipoprotein (HDL) concentrations in human plasma samples were measured on an Abbott Architect ci8200 analyzer in the St. Louis University Hospital Clinical Core Laboratory, a Clinical Laboratory Improvement Amendments–certified, College of American Pathologists–accredited laboratory. Total LDL was calculated using the Friedewald equation [LDL = Total cholesterol − HDL cholesterol − Triglyceride/5].

Mice

C57BL/6 mice were purchased from Jackson laboratory (catalog no. 000664). Splenocytes from Pmel transgenic mice (Jackson laboratory, catalog no. 005023) were obtained from Guanyong Peng (Saint Louis University, St. Louis, MO). All mice were housed under specific pathogen–free conditions and used in accordance with protocols approved by the Institutional Animal Care and Use Committee of the Department of Comparative Medicine, Saint Louis University School of Medicine (St. Louis, MO).

Tumor cell lines and immunotherapy

The B16-F0 melanoma cell line was purchased from ATCC (catalog no. CRL-6322) in 2019. FBL (Friend virus–induced erythroleukemia of B6 origin) leukemia and TRAMP (transgenic adenocarcinoma of mouse prostate) prostate cancer cell lines were obtained from Phil Greenberg (University of Washington, Seattle, WA) in 2009. The MC38 colon carcinoma cell line was obtained from Guanyong Peng (Saint Louis University, St. Louis, MO). The E0771 breast cancer cell line was obtained from Ratna Ray (Saint Louis University, St. Louis, MO) in 2018. The human melanoma line A375 was purchased from ATCC (catalog no. CRL-1619) in 2019. All tumor lines were confirmed negative for *Mycoplasma* on February 2, 2020 by PCR using a kit from ATCC (catalog no. 30-1012K) according to the manufacturer's protocol. Tumor cell lines were maintained in DMEM (Thermo Fisher Scientific, catalog no. 11995-065) supplemented with 10% FBS and 1% Pen/Strep (Sigma-Aldrich, catalog no. P0781). Adherent cells were removed with 0.25% trypsin and cells passaged 3–5 times for each experiment. For B16-F0 studies, 1×10^6 tumor cells were injected subcutaneously into both flanks. For E0771 study, 1×10^6 tumor cells were injected in the mammary fat pad. Mice were treated intraperitoneally with 5 mg/kg of anti-PD1 (RMP1-14) from Bio X Cell (catalog no. BE0146) on days 6, 10, and 14 with or without intraperitoneal treatment with an HO-1 inhibitor, OB24 from TOCRIS (catalog no. 6119) at 30 mg/kg on days 3, 6, 8, and 12. Digital calipers were used to measure tumor dimensions and calculate volume in mm^2 using the equation $(L \times W^2)/2$. Spleens and tumor tissues were mechanically disrupted using a sterile 3 mL syringe plunger and single-cell suspensions prepared in DMEM containing 10% FBS and 1% Pen/Strep prior to analysis.

Flow cytometry

Flow cytometric analysis was performed on an LSR II and an LSR Fortessa FACS analyzer (BD Biosciences) in the Saint Louis University (St. Louis, MO) Flow Cytometry Core Facility. Live lymphocytes were identified as negative for live/dead stain (Thermo Fisher Scientific, catalog no. L34966A) and positive for staining with anti-CD45 (BioLegend, clone HI30, catalog no. 304042). These were segregated into $CD4^+$ and $CD8^+$ T cells, $CD4/8^-$ $CD19^+$ B cells and $CD56^+$ natural killer (NK) cells after staining with anti-CD8 (clone SK1, catalog no. 344714), anti-CD4 (clone RPA-T4, catalog no. 300526), anti-CD19 (clone HIB19, catalog no. 302206). and anti-CD56 (clone HCD56, catalog no. 318336), all purchased from BioLegend. $CD4^+$ T cells were further segregated into conventional $FoxP3^-$ and $Foxp3^+$ regulatory cells using anti-FoxP3 (clone 259D/C7, catalog no. 562421) from BD Biosciences. Intracellular cytokine staining was performed using the Cytofix/Cytoperm Plus Kit (BD Biosciences, catalog no. BD 554714) according to the manufacturer's instructions following *ex vivo* stimulation with phorbol 12-myristate 13-acetate and Ionomycin for 4 hours in the presence of GolgiPlug (BD Biosciences, catalog no. 52-2301KZ). Intracellular antibodies, anti-IFNγ (clone B27, catalog no. 506507) and anti-TNF (clone MAb11, catalog no. 502930), granzyme B (clone QA16A02, catalog no. 372208), Perforin (clone dG9, catalog no. 308126), and Ki67 (clone Ki-67, catalog no. 350512) were purchased from BioLegend. Anti–T-bet (clone eBio4B10) was purchased from eBioscience (catalog no. 50-5825-82). Other antibodies specific for human cell surface antigens were anti-CD39 (clone A1, catalog no. 328228) and anti-CD279/PD1 (EH12.2H7, catalog no. 329927) from BioLegend, and anti-CD103 (clone B-Ly7) from Invitrogen (catalog no. 4330509). All analysis on human cells was performed directly after cell thawing multiple patient samples simultaneously to avoid day-to-day variability. Mouse cells were stained with antibodies against CD8 (clone 53-6.7, catalog no. 100714), granzyme B (clone GB11, catalog no. 515403), Ki67 (clone 16A8, catalog no. 652413), and IFNγ (clone: XMG12, catalog no. 505808) from BioLegend. All flow cytometry data were analyzed using FlowJo v.10 software (Tree Star Inc.).

Western blot analysis

Tumor cells were lysed in 1× lysis buffer from Cell Signaling Technology (catalog no. 9803) augmented with protease and phosphatase inhibitors from Cell Signaling Technology (catalog no. 5872S). Proteins were size separated by electrophoresis on precast 4%–12% Bis-Tris gels (Invitrogen, catalog no. NP0321BOX) and transferred on to nitrocellulose membranes (Invitrogen, catalog no. LC2001). All antibodies were purchased from Cell Signaling Technology. HO-1 protein was detected by anti-mouse HO-1 (E6Z5G, catalog no. 82206S) or anti-human HO-1 (E3F4S, catalog no. 43966S) diluted from the manufacturer's stock 1:1,000 in Tris-buffered saline and 0.1% Tween-20 (Thermo Fisher Scientific, catalog no. CAS9005-64-5). Primary antibody was detected with horseradish peroxidase–linked anti-rabbit IgG (catalog no. 7074) and β-actin detected with a cross-reactive anti-mouse/human (clone 13E5, catalog no. 5125S) diluted 1:5,000. Western blots were visualized by chemiluminescence using ECL reagent from Cell Signaling Technology (catalog no. 6883S) according to the manufacture's protocol. Densitometry was performed using ImageJ software.

Apoptosis assay

Human A375 melanoma tumor cells were pretreated for 4 hours in culture medium with 10 μg/mL of ox-LDL (Kalen Biomedical LLC, catalog no. 7702026) or LDL (Lee Biosolutions Inc, catalog no. 360–25–1) in the presence or absence of the HO-1 inhibitor, OB24 (TOCRIS, catalog no. 6119) at 30 μg/mL. After 4 hours, doxorubicin (Fresenius Kabi, catalog no. 62653) was added to a final concentration of 10 μmol/L and cells were incubated overnight at 37°C. Cells were permeabilized and stained with CaspGlow Fluorescein Active Caspase Staining Kit from Invitrogen (catalog no. 88-7003) and Annexin V (catalog no. A35110) according to the manufacturer's protocol and analyzed by flow cytometry. For mouse tumors, splenic T cells from naïve Pmel mice were processed into a single-cell suspension at 1×10^6 cells/mL, and stimulated with 4 μg/mL anti-CD3 (eBioscience, catalog no. 14-0032-85) and 4 μg/mL anti-CD28 (BioLegend, catalog no. 102102) for 72 hours. B16 melanoma cells were pretreated with 10 μmol/L Hemin (Sigma-Aldrich, catalog no. 51280) or 4 μg/mL of either LDL or ox-LDL for 48 hours. Splenocytes and B16 cells were then cocultured at a 10:1 effector to target ratio for 72 hours. Tumor cell apoptosis was assessed by staining for pan-caspase (CaspGlow Invitrogen, catalog no. 88-7003-4), and Annexin V (Invitrogen, catalog no. A35110) according to the manufacturer's protocol and analyzed by flow cytometry.

Statistical analysis

Kaplan–Meier curves were used to analyze PFS and overall survival (OS). Comparisons of patient cohorts stratified by BMI, plasma LDL concentration or *HMOX1* gene expression was performed with a log-rank (Mantel–Cox) test. Statistical analyses to compare multiple cell populations were performed using an unpaired, two-tailed, nonparametric Mann–Whitney *U* test (Prism 7.0, GraphPad Software). Linear regression analysis to assess correlation between two parameters was performed by calculating the Pearson value (*r*) and the corresponding *P* value for *r* using Prism 7.0. Exact *P* values are provided when available.

Results

Survival of patients with cancer receiving immunotherapy is not predicted by BMI

In 2010, Hodi and colleagues published results from a landmark clinical trial, NCT00094653, showing improved OS among patients with metastatic melanoma receiving ipilimumab (anti-CTLA4) checkpoint blockade immunotherapy (17). We performed a retrospective analysis using these data in which we compared BMI with PFS and OS for the 129 patients treated with ipilimumab monotherapy. When patients were stratified into those with a BMI above 30 (obese) and those with a BMI below 30 (not obese), there was no correlation between PFS and BMI (Supplementary Fig. S1). However, patients in the obese cohort showed a slight increase in OS (**Fig. 1A**), stemming mostly from improved OS among obese male but not female patients treated with ipilimumab (Supplementary Fig. S2), which is consistent with another report (8). These results suggest that the mechanisms linking obesity and altered responses to immunotherapy are still not well understood.

To determine whether BMI had a greater influence on outcomes after immunotherapies targeting PD1 or PDL1, we performed a second retrospective analysis of 149 patients with various cancer types treated at our institution with either anti-PD1 (nivolumab or pembrolizumab) or anti-PDL1 (atezolimumab or durvalumab; Supplementary Table S1). In contrast to the ipilimumab analysis above, patient OS was independent of BMI (**Fig. 1B**). Obese female patients had a slightly better response to immunotherapy than leaner women but this difference in OS did not reach the threshold of statistical significance (Supplementary Fig. S2). Survival among men treated with anti-PD1/L1 was essentially identical for the two BMI groups (Supplementary Fig. S2). Overall, these two clinical studies suggest there is no obvious connection between BMI and patient outcomes after checkpoint blockade immunotherapy.

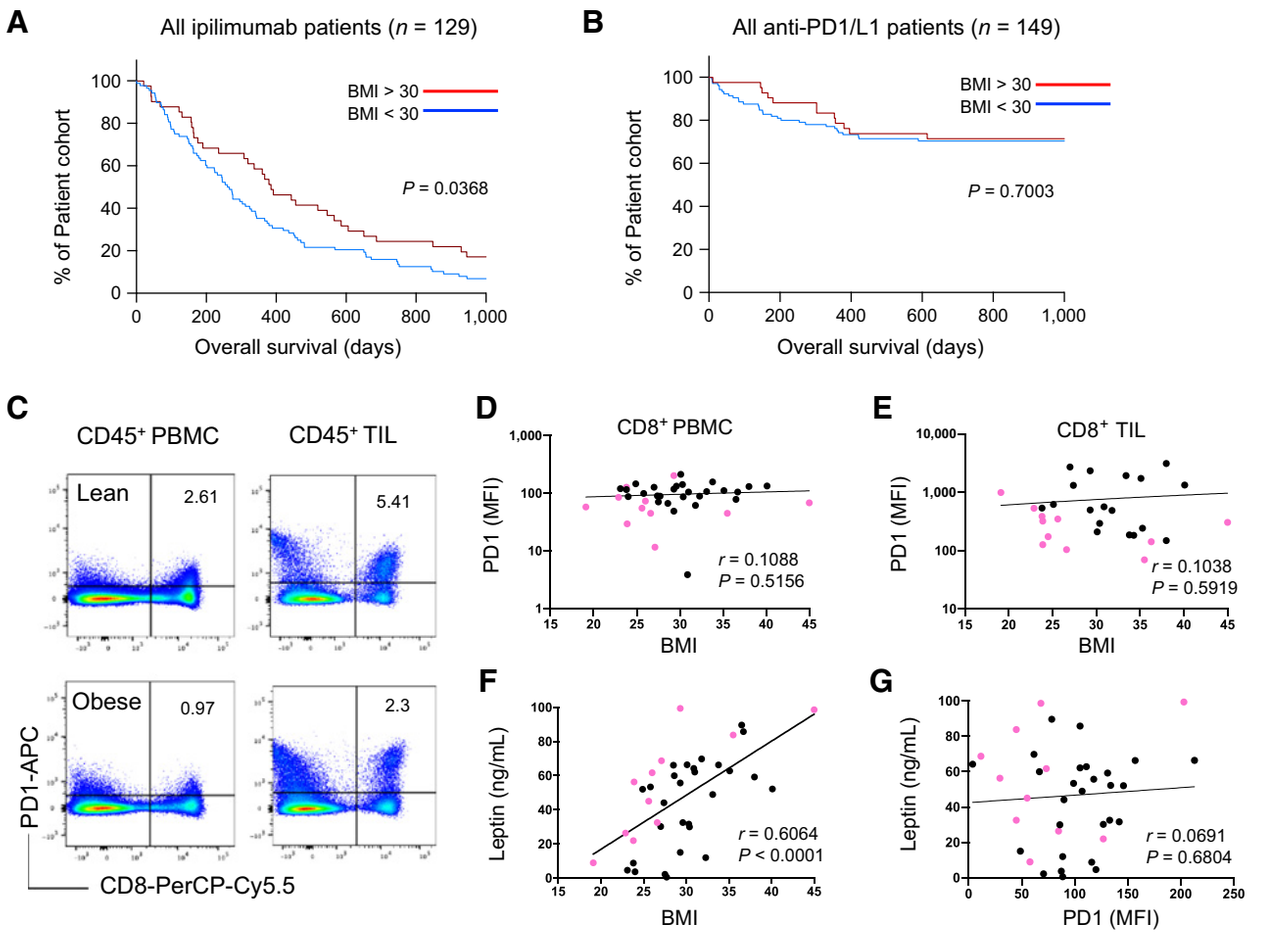

Figure 1.

Obesity and leptin levels do not accurately predict responses to checkpoint blockade immunotherapy. Retrospective analysis of patient survival after treatment with the anti-CTLA4 ipilimumab or anti-PD1/anti-PDL1. Kaplan–Meier curves show OS data for 129 patients with melanoma treated with anti-CTLA4 (**A**) and 149 patients with various cancers treated with anti-PD1 or anti-PDL1 (**B**). Patient-derived PBMCs and TILs were analyzed by flow cytometry and gated on $CD45^+$ live cells. **C,** Representative FACS plots from lean (top) and obese (bottom) patients show PD1 surface expression on $CD8^+$ PBMCs (left) and $CD8^+$ TILs (right). Linear regression analysis of PD1 MFI on $CD8^+$ PBMCs (**D**) and TILs (**E**) from 27 patients with melanoma (black circles) and 11 patients with breast cancer (pink circles) versus BMI. Correlative analysis of plasma leptin concentration versus BMI (**F**) or PD1 MFI (**G**) on $CD8^+$ PBMCs from these same patients is shown, with inset numbers indicating the *r* values for each dataset along with corresponding *P* values.

Increased leptin in obese patients does not influence PD1 expression or T-cell function

To understand the possible discrepancy between our results and the PD1/leptin paradigm (9), we sought to confirm the link between leptin and PD1 expression in patients with cancer. This could not be directly investigated in any of our retrospective clinical cohorts because biological samples were not accessible. Instead, we initiated a prospective study to measure PD1 expression on PBMCs derived from patients with cancer. PBMCs were isolated from 27 patients with melanoma and 11 patients with breast cancer receiving standard-of-care treatment at Saint Louis University Hospital (St. Louis, MO). Flow cytometric analysis showed relatively low PD1 surface expression on peripheral $CD8^+$ T cells from all patients, which was unaffected by donor BMI when compared by mean fluorescence intensity (MFI; **Fig. 1C** and **D**) or when the frequency of $PD1^+$ $CD8^+$ and $CD4^+$ T cells was compared with BMI (Supplementary Fig. S3). To confirm that our inability to connect BMI with PD1 expression did not reflect some laboratory or cohort-specific anomaly, we augmented our data with additional samples from 30 patients with non-Hodgkin lymphoma that were not treated with checkpoint inhibitors and 21 healthy volunteers analyzed independently by two different collaborators in their respective laboratories. These analyses showed no correlation between patient BMI and PD1 expression on T cells (Supplementary Fig. S4).

In patients where tumor tissue was available, we observed greater overall expression of PD1 on $CD8^+$ TILs compared with PBMCs, but PD1 expression was unrelated to patient BMI (**Fig. 1C** and **E**). These results were not due to low leptin levels, which were significantly elevated in the plasma of obese patients and correlated closely with BMI (**Fig. 1F**), as previously reported by others (18). However, leptin did not associate positively or negatively with expression of PD1 on human $CD8^+$ T cells (**Fig. 1G**). This seemingly controversial finding is not altogether surprising given that other leptin studies have produced highly disparate results, suggesting that leptin can both increase and decrease PD1 expression on T cells (9, 19) and has both positive and negative effects on T-cell function (10, 20–24). Here, we addressed this question in a diverse population of patients with cancer and healthy donors from different institutions, finding no evidence of a link between obesity-associated leptin and expression of PD1 on either peripheral or tumor-infiltrating T cells. Our data suggest that the proposed paradigm between leptin and T-cell suppression via PD-1 is not broadly applicable and therefore does not represent a reliable tool for predicting patient outcomes.

To investigate whether obesity was associated with functional immune suppression, regardless of PD-1 expression levels, we examined peripheral immune responses in patients with melanoma with a range of BMI. PBMCs from patients with melanoma were first examined for frequencies of T cells, B cells, and NK cells but showed no differences among the two cohorts (Supplementary Fig. S5). The functional potential of $CD8^+$ T cells was determined by measuring expression the effector molecules perforin and granzyme B and production of the cytokines IFNγ and TNF after 4-hour *ex vivo* restimulation. We observed a variety of functional responses based on these metrics but none correlated statistically with BMI (Supplementary Fig. S5). Similar assessment of $CD4^+$ T cells was consistent with these results (Supplementary Fig. S6), providing further evidence that functional responses by peripheral T cells in patients with cancer operate independently of BMI.

Serum lipids are associated with impaired T-cell immune responses in patients with cancer

As a metric of human obesity, BMI is quite limited and accounts only for height and weight. The question remains whether different and perhaps more nuanced biometrics associated with obesity, diet, and metabolic health could better predict patient outcomes after treatment with checkpoint blockade immunotherapy. To begin addressing this question, we established a composite score to gauge functional immune potential across patient populations. This immune score was calculated for individual patients by adding the percentage of granzyme B/perforin double-positive $CD8^+$ PBMCs plus the percentage of IFNγ/TNF double-positive $CD8^+$ PBMCs induced after restimulation. The PBMC data used to generate the immune scores for patients with melanoma and breast cancer are reported in Supplementary Fig. S5. As expected from our earlier results, neither BMI nor plasma leptin levels correlated with this functional immune score (**Fig. 2A** and **B**).

Moving beyond BMI and plasma leptin levels, differences in metabolic health have the potential to impact immune function and we anticipated these may be detected by lipidomic assessment. Analysis of plasma samples from these same patients with melanoma and breast cancer revealed an abundance of total cholesterol and LDL associated with a reduced immune score, independent of BMI (**Fig. 2C** and **D**). HDL showed a similar trend but did not reach statistical significance (**Fig. 2E**). Much of what is understood about the complex intersection between immunity and serum lipids has come from the study of atherosclerosis where the immune system plays a complex and dynamic role in disease (25). By the late 1980s, oxidative stress and subsequent ox-LDL were recognized as important factors in regulating plaque formation and immune cell function (26, 27). Later work uncovered a potentially inhibitory influence of cholesterol and ox-LDL on T cells (25, 28, 29), which could explain why LDL levels correlated with low immune scores in our patients. Whether these mechanisms are operative in clinical cancer biology or tumor immunity remains unknown.

To gauge the possible influence of ox-LDL on patient immune score, we initially quantified CE by mass spectrometry, as CE represents a sentinel lipid species known to be induced by ox-LDL (27, 30). Plasma CE concentrations were inversely associated with immune score (**Fig. 2F**), nearly overlapping with total cholesterol and LDL profiles in the same patients (**Fig. 2C** and **D**). Direct quantification of ox-LDL by ELISA confirmed this, revealing a clear inverse correlation with $CD8^+$ T-cell function (**Fig. 2G**). The level of ox-LDL also closely correlated with total cholesterol and total LDL (**Fig. 2H**), which carries clinical importance as these molecules are commonly assessed in patients and could be employed as reasonable surrogate markers for ox-LDL. Patient BMI did not correlate with concentrations of plasma cholesterol, LDL or ox-LDL (Supplementary Fig. S7). To determine whether these lipidomic profiles were predictive of therapeutic outcomes, we accessed the retrospective OS data from patients treated with anti-PD1/L1 (**Fig. 1B**). Of the 149 patients, only 30 had serum lipid data available for analysis. Despite this reduced number, when patients were stratified into high and low LDL cohorts (which overlapped with high and low cholesterol), OS was inversely correlated with plasma LDL concentrations (**Fig. 2J**). This result supports the well-documented associations between cholesterol, tumor immunity, and cancer progression (29, 31–33). The question remains how such changes in serum lipids intersect mechanistically with responses to checkpoint blockade immunotherapy.

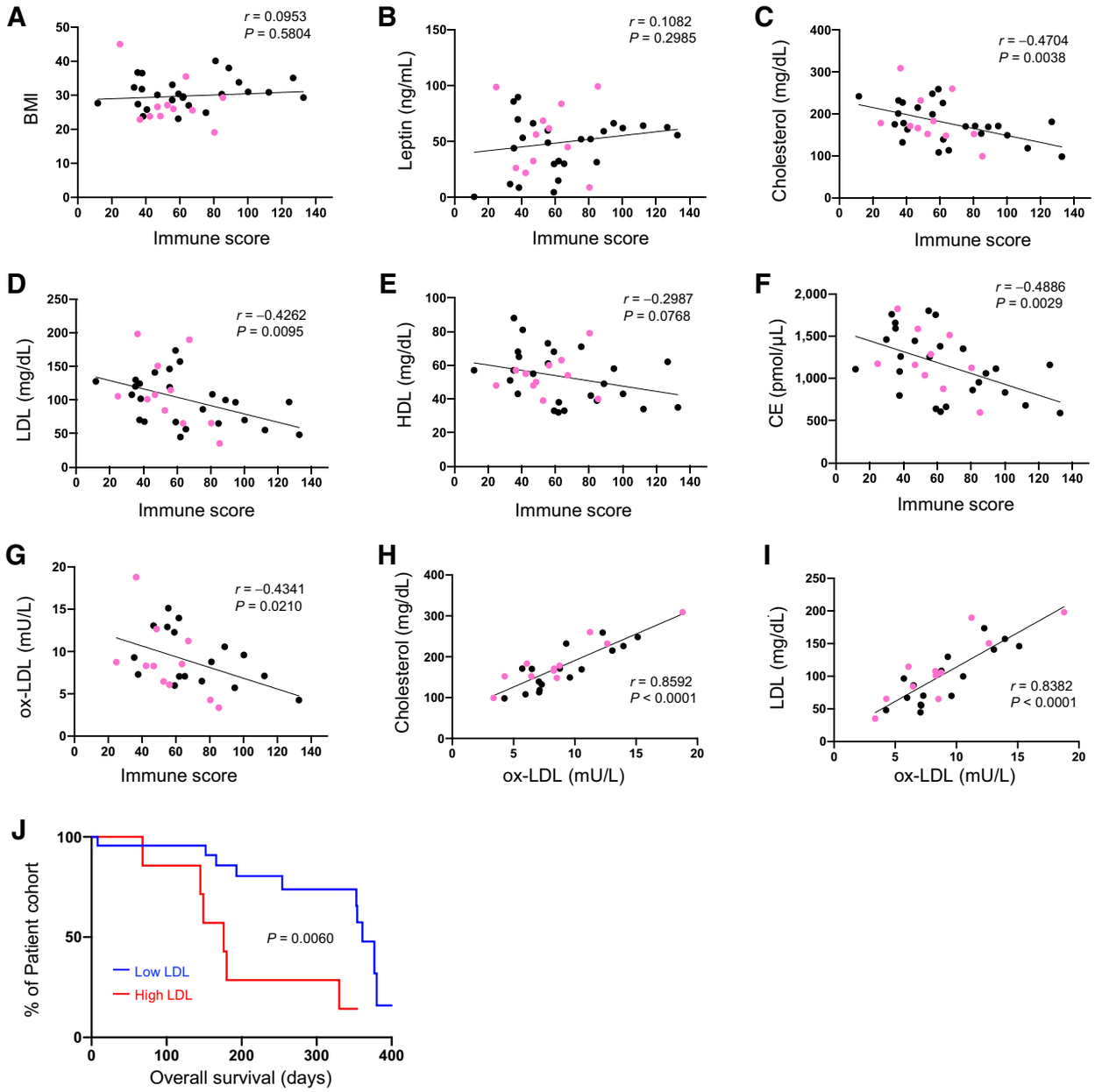

Figure 2.

Patient immune function correlates with lipid profile independent of BMI and leptin. Serologic analysis of plasma samples from patients with melanoma (black) and breast cancer (pink). Graphs display linear regression of patient BMI (**A**), leptin (**B**), total cholesterol (**C**), LDL (**D**), HDL (**E**), and CE (**F**) versus immune score for 25 patients with melanoma and 11 patients with breast cancer. Linear regression of patient ox-LDL versus immune score (**G**), cholesterol (**H**), and LDL (**I**) for 17 patients with melanoma and 11 patients with breast cancer. Each circle represents data from an individual patient, with inset numbers showing *r* values for each dataset along with corresponding *P* values. **J,** Kaplan–Meier curves display OS data for 30 patients with cancer stratified by plasma LDL concentration treated with anti-PD1/L1.

The clinical analysis above established a correlation between serum cholesterol (LDL and ox-LDL) and reduced $CD8^+$ T-cell immune function. To determine whether LDL and ox-LDL had a direct effect on human T-cell function, PBMCs from 10 healthy donors were stimulated with anti-CD3 for 6 days in the presence or absence of LDL or ox-LDL. Those stimulated in the presence of ox-LDL showed lower frequencies of $CD8^+$ T cells whereas LDL had essentially no impact (**Fig. 3A**). This likely reflected an impairment in proliferation, as detection of Ki67 in $CD8^+$ T cells stimulated in the presence of ox-LDL was significantly reduced (**Fig. 3A**). Reduced proliferation was consistent among the donors, and although responses varied in magnitude, 9 of 10 donors showed lower Ki67 expression among $CD8^+$ T cells stimulated in the presence of ox-LDL (**Fig. 3B**). This loss of proliferative capacity was not observed in $CD4^+$ PBMCs (**Fig. 3A**), suggesting the inhibitory influence of ox-LDL was uniquely potent for $CD8^+$ T cells. Compounding the impact of low $CD8^+$ T-cell

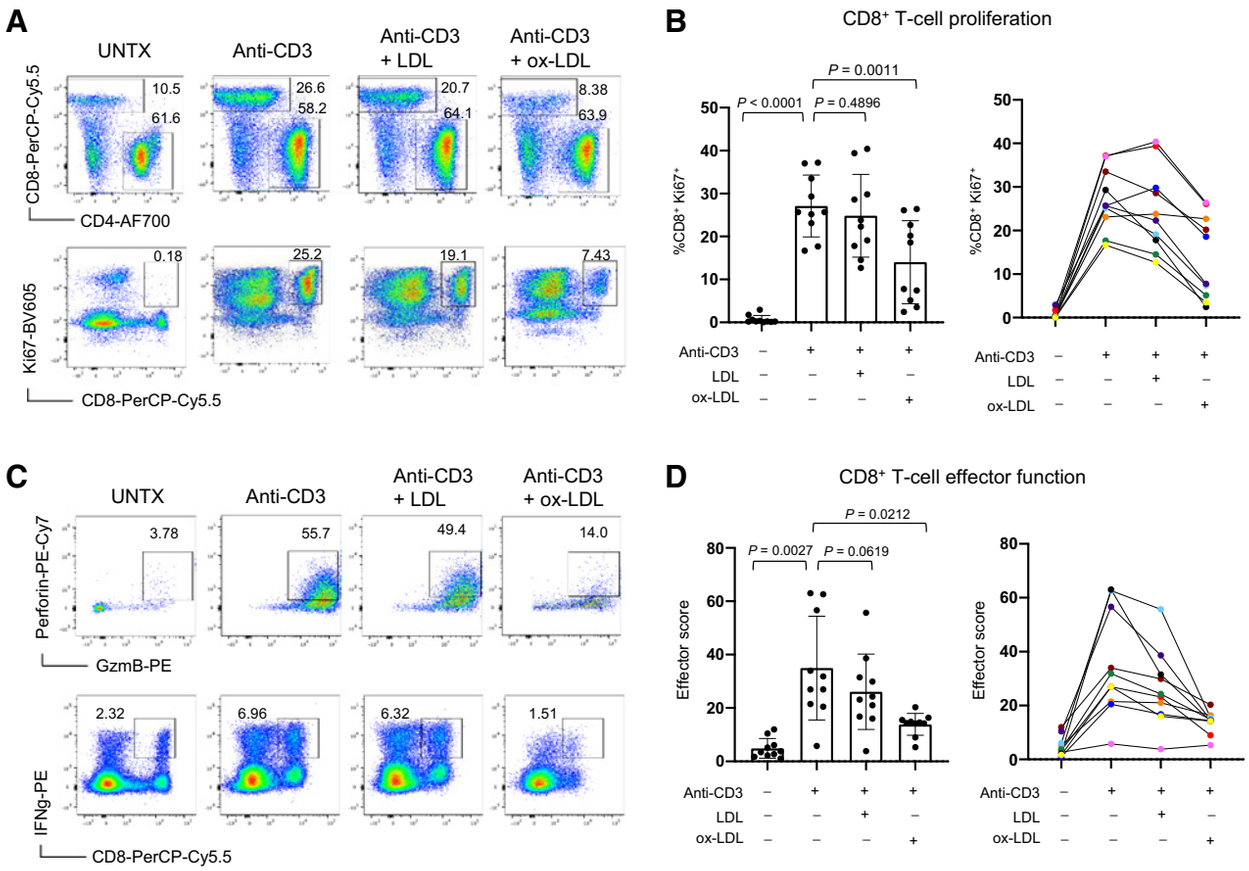

Figure 3.

ox-LDL inhibits human CD8$^+$ T-cell proliferation and effector responses. Human PBMCs were stimulated with anti-CD3 for 6 days. **A,** Representative FACS plots show CD8$^+$ and CD4$^+$ T cells among all CD45$^+$ lymphocytes (top) and Ki67$^+$ CD8$^+$ cells (bottom) gated on CD45 expression. Inset numbers indicate the percentage of total CD45$^+$ cells within the incribed regions. **B,** Graphs show percentage of Ki67$^+$ CD8$^+$ T cells from the indicated treatment groups (left) and as individual responses traced for each donor in a different color (right). **C,** Representative FACS plots show the frequency of granzyme B (GzmB) and perforin expression among all CD45$^+$ CD8$^+$ T cells (top) and IFNγ production by CD8$^+$ T cells after restimulation (bottom). **D,** Graphs show the cumulative effector score for indicated treatment groups (left) and individual responses for each donor (right). All graphs show data from the same 10 donors, where each dot represents data from an individual donor and each color follows responses by a single donor over the four treatments. Exact *P* values are provided for the bracketed groups, and error bars represent SEM.

frequencies, ox-LDL also impaired CD8$^+$ T-cell function as measured by expression of granzyme B, perforin, and production of IFNγ (**Fig. 3C**). For a broader assessment of impaired effector function, we added the frequencies of all CD8$^+$ T cells expressing high granzyme B, perforin and IFNγ together to create an effector score for all 10 donors. These scores illustrate the extent of CD8$^+$ T-cell dysfunction resulting from exposure to ox-LDL during activation (**Fig. 3D**). These data support our clinical results from patients with cancer (**Fig. 2G**), suggesting that high serum lipoproteins, and ox-LDL in particular, are immunosuppressive with the potential to provide resistance against immune-based treatment strategies.

Lipoproteins induce tumor cytoprotective mechanisms and resistance to immunotherapy

High levels of serum LDL, and especially ox-LDL in particular, also have the potential to impact tumor cells directly. Elevated cholesterol, lipids, and ox-LDL stimulate production of reactive oxygen species and increase oxidative stress (34, 35). A major cellular response to oxidative stress is increased expression of the cytoprotective molecule HO-1, encoded by *HMOX1*, which is also induced in a variety of human cells in response to oxidatively modified lipids (36). Originally recognized for its role in oxidative degradation of heme to biliverdin, HO-1 also promotes cellular survival under conditions of stress (37). This activity is vital for protection of healthy tissues, but when HO-1 expression is increased in cancer, it can render tumor cells more resistant to endogenous immune responses and therapeutic interventions, as we and others have demonstrated (23, 38–40). Indeed, data retrieved from the GEPIA database showed a strong negative correlation between human HO-1 expression and melanoma patient survival, and a positive correlation with advanced disease stage indepdent of treatment (**Fig. 4A**).

To determine whether HO-1 expression is influenced by LDL and ox-LDL, B16 mouse melanoma cells were maintained under culture conditions with various concentrations of these lipoproteins. After 3 days, expression of HO-1 protein was evident in all samples and increased in the presence of LDL and ox-LDL (**Fig. 4B**). This was particularly true for the truncated 28 kDa form, which is important for transcriptional activation of genes involved in the response to oxidative stress (41). This response to LDL and ox-LDL was partially recapitulated in A375 human melanoma cells, but only the 32 kDa

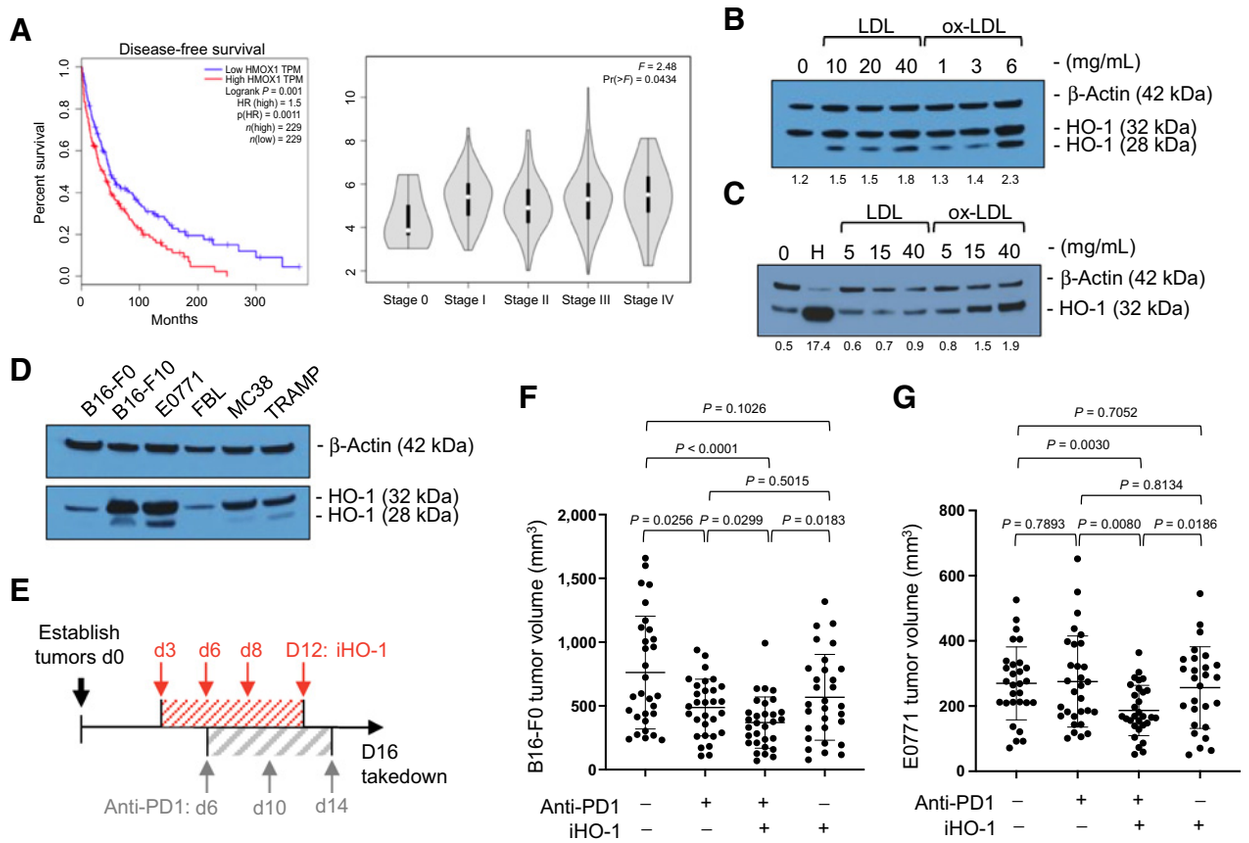

Figure 4.

HO-1 is negatively associated with patient survival and promotes resistance to immunotherapy. **A,** Melanoma patient survival and disease stage relative to tumor *HMOX1* gene expression data obtained from the GEPIA. A total of 458 patients with melanoma (229 high and 229 low) were analyzed independent of treatment, and the indicated *P* value between these groups was determined by a log-rank test. HO-1 protein expression in mouse B16-F0 cells (**B**) and human A375 melanoma tumor cells (**C**) incubated with the indicated concentration of LDL, ox-LDL, or H-hemin were analyzed for HO-1 and β-actin expression by Western blot analysis. Densitometry results shown below each band indicate the ratio of total HO-1 to β-actin and data shown are representative of three independent experiments. **D,** HO-1 protein expression in various murine tumor lines measured by Western blot analysis. **E,** Diagram of experimental setup where mice with established B16-F0 melanoma or E0771 breast tumors were treated with anti-PD1 on days 6, 10, and 14 with or without treatment with an HO-1 inhibitor (iHO-1: OB24) on days 3, 6, 8, and 12. **F,** Subcutaneous bilateral B16-F0 tumor volumes (mm^3) on day 16 are shown for 15 mice (30 tumors) per treatment group pooled from three independent experiments. **G,** E0771 tumor volume (mm^3) in mammary fat pads on day 16 are shown for 14 mice (28 tumors) per treatment cohort pooled from three different experiments. Exact *P* values are provided for the bracketed groups, and error bars represent SEM.

form was detected here (**Fig. 4C**). Together, these results demonstrate the potential of LDL and ox-LDL to induce cytoprotective HO-1 in melanoma tumors.

Tumor HO-1 expression promotes resistance to immunotherapy

In murine melanoma, HO-1 expression promotes tumor cell proliferation and disease progression (42), suggesting HO-1 may be a mechanism of therapeutic resistance. We observed highly variable expression of HO-1 among different murine tumor cell lines grown in culture (**Fig. 4D**). To determine whether expression of HO-1 provided melanoma tumors with resistance to immunotherapy, mice with 6-day established subcutaneous B16-F0 tumors were treated with anti-PD1 on days 6, 10, and 14 with or without simultaneous treatment with an HO-1 inhibitor (iHO-1), OB24 (38) on days 3, 6, 8, and 12 (**Fig. 4E**). We and others have previously shown that B16 melanoma is partially resistant to checkpoint blockade immunotherapy (43, 44), but treatment here with anti-PD1 alone resulted in significantly smaller melanoma tumors by day 16 (**Fig. 4F**). Although treatment with iHO-1 alone had little impact on tumor size, the combination regimen produced an additive antitumor effect, resulting in smaller tumors compared with those treated with either monotherapy. To test this treatment strategy on tumors with higher endogenous HO-1 expression, female mice bearing E0771 breast tumors in the mammary fat pad were examined. Unlike melanoma, these breast tumors were completely refractory to monotherapy with either anti-PD1 or iHO-1 (**Fig. 4G**). However, mice treated with the combination had significantly smaller tumors by day 16. These proof-of-principle *in vivo* studies suggest tumors with high HO-1 expression are more resistance to anti-PD1 immunotherapy but this can be overcome by inhibition of HO-1.

Previous studies have suggested that inhibition of HO-1 may improve immune cell function (39), which could explain the therapeutic efficacy of combination anti-PD1 plus iHO-1. To determine whether this was the case in mice treated with OB24, we examined $CD8^+$ TILs from differentially treated mice. Anti-PD1 treatment resulted in higher frequencies of $CD8^+$ T cells infiltrating melanoma tumors, but this was true regardless of HO-1 inhibition (**Fig. 5A**).

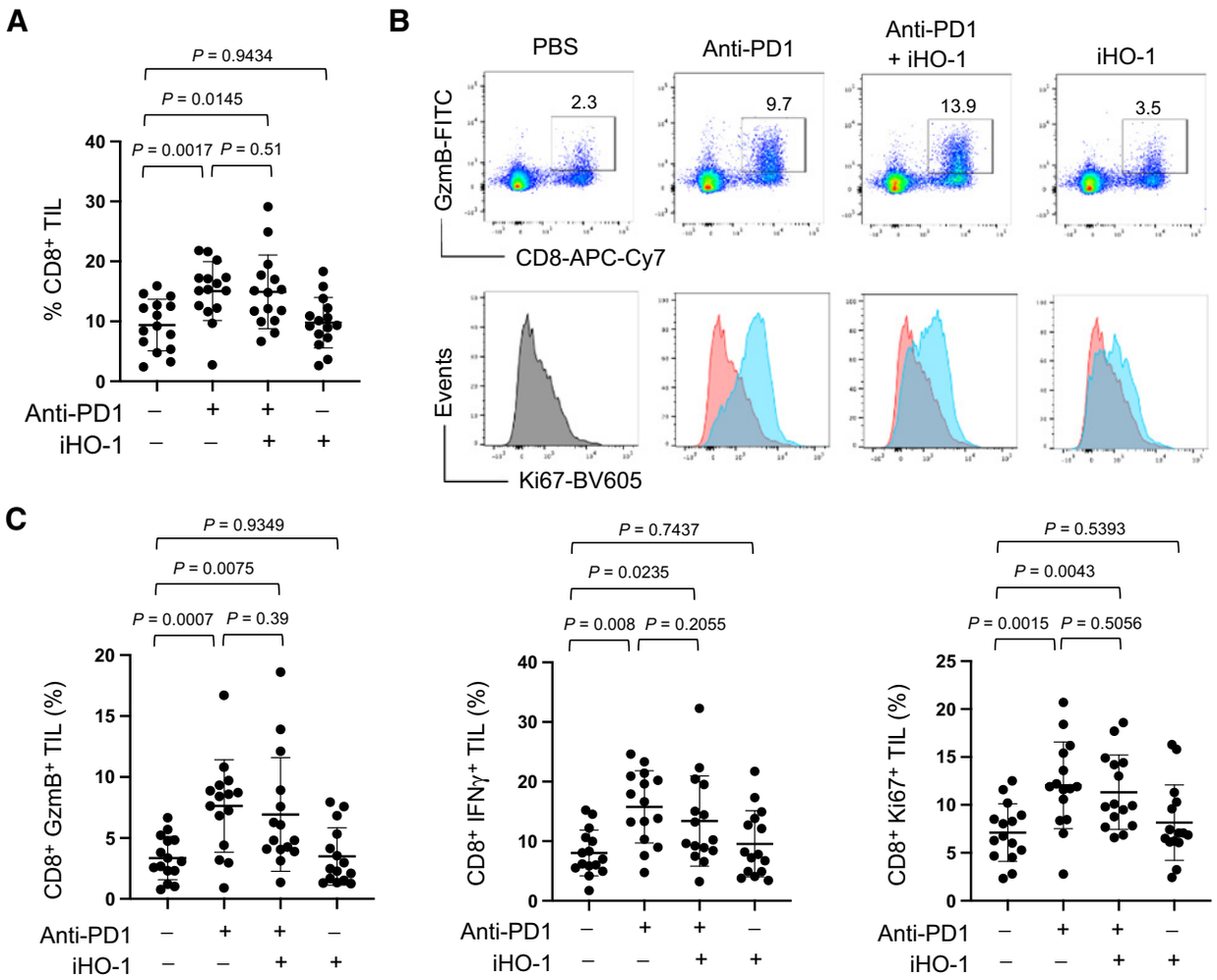

Figure 5.

Inhibition of HO-1 overcomes resistance to immunotherapy independent of CD8$^+$ TIL function. B6 mice bearing B16-F0 melanoma tumors were treated as described in **Fig. 4E**, and TILs were assessed on day 16. **A,** Frequency of CD8$^+$ TILs from 15 mice per treatment cohort pooled from three independent experiments. **B,** Representative FACS plots show granzyme B (GzmB) expression (top) and histograms show Ki67 expression (bottom) of CD8$^+$ TILs for the different treatment groups in blue relative to PBS control in red. **C,** Frequency of CD8$^+$ TILs expressing GzmB, IFNγ, and Ki67 is shown for each treatment group, and data are pooled from three independent experiments, with each point representing data from an individual mouse. Exact *P* values are provided for the bracketed groups, and error bars represent SEM.

Functional assessment of CD8$^+$ TILs showed similar expression of granzyme B and equivalent proliferation (Ki67) elicited by either anti-PD1 alone or in combination with iHO-1 (**Fig. 5B**). Pooled responses demonstrated these same trends across multiple experiments assessing granzyme B, IFNγ, or Ki67 expression among CD8$^+$ TILs (**Fig. 5C**). We interpret these data as evidence that systemic HO-1 inhibition, at least with the OB24 reagent, did not impact antitumor immunity directly. Rather, our results imply that the enhanced tumor control observed in combination-treated mice (**Fig. 4F** and **G**) likely stemmed from inhibition of the cytoprotective functions of HO-1 within tumor cells, making them more susceptible to immune-mediated killing.

The cytoprotective role of HO-1 is well documented for healthy tissues (45) and has been identified as a potential barrier to treatment of several cancers (38, 40, 46). Because LDL and ox-LDL induced HO-1 expression in human tumors (**Fig. 4C**), we directly tested whether these serum lipoproteins could protect human melanoma cells from apoptosis. A375 cells were treated with doxorubicin to induce apoptosis overnight along with LDL, ox-LDL, or a known inducer of HO-1 (hemin) in the presence or absence of the iHO-1. Apoptosis was assessed by expression of active caspase and Annexin V staining. Treatment with doxorubicin induced approximately 20% of cells to become apoptotic (double-positive) compared with less than 1% of control cells treated with PBS (**Fig. 6A**). These human melanoma cells were nearly completely shielded from doxorubicin-induced apoptosis when HO-1 was induced by treatment with hemin, indicating that high HO-1 expression provides strong protection from otherwise potent inducers of cell death. Exposure to LDL or ox-LDL also provided a certain level of cytoprotection, reducing the frequency of apoptotic cells by approximately half (**Fig. 6B**). This cytoprotection was reliant on HO-1 as treatment with iHO-1 brought the frequency of apoptotic cells back to levels observed with doxorubicin alone. To determine whether LDL and ox-LDL protected melanoma cells specifcally from

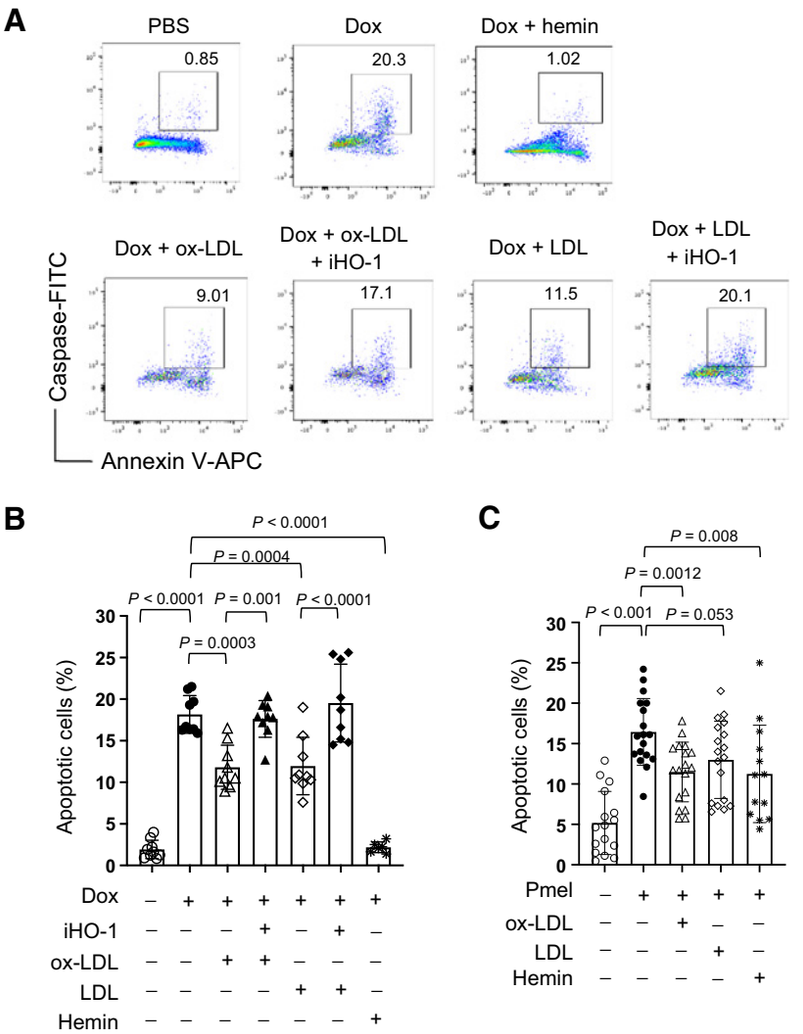

Figure 6.

ox-LDL and LDL induce HO-1–mediated cytoprotection in human melanoma tumors. A375 human melanoma cells were pretreated for 4 hours with ox-LDL, LDL, or hemin in the absence or presence of iHO-1 (OB24; 30 μg/mL) and then treated with doxorubicin (Dox) for 24 hours. Representative FACS plots show expression of active caspase (CaspGlow) and Annexin V in A375 tumor cells (**A**), and the percentage of double-positive cells (**B**) is shown for the different treatment groups with data pooled from three independent experiments. **C,** B16 melanoma cells were pretreated with 10 μmol/L hemin, LDL, or ox-LDL for 48 hours and then cocultured with activated Pmel T cells at a 10:1 effector-to-target ratio for 3 days. Tumor cell apoptosis was assessed by active caspase and Annexin V staining, and percentage of double-positive cells is graphed for the different treatment groups with data pooled from three independent experiments. Each point represents data from an individual replicate well, with exact *P* values provided for the bracketed groups and error bars representing SEM.

$CD8^+$ T cell–mediated killing, B16 tumors were pretreated with LDL or ox-LDL and then cultured with activated tumor-specific Pmel T cells. In the absence of intervention, increased apoptosis was evident in B16 cells exposed to Pmel $CD8^+$ T cells (**Fig. 6C**). However, tumor cells pretreated with LDL, ox-LDL, or hemin were partially resisted to T cell–induced apopotosis. Extrapolation of these data predicts that higher levels of ox-LDL and LDL in patient serum may induce HO-1 expression sufficient to resist treatment-mediated apoptosis, making these tumors more challenging for T cells to kill. Given the association between high HO-1 expression and poor survival of patients with melanoma (**Fig. 4A**), our results encourage further exploration of HO-1 as a therapeutic target in combination with checkpoint blockade to extend the success of cancer immunotherapy to patients that might otherwise be classified as nonresponders, particularly in patients with high serum cholesterol and LDL.

Discussion

The U.S. Center for Disease Control and Prevention estimates that nearly 40% of Americans are obese. Among the many health concerns associated with obesity is an increased risk of developing certain types of cancer such as esophageal, colon, renal, and endometrial cancers (47). Weaker correlations have also been noted for malignant melanoma, breast cancer, leukemias, and lymphomas (48, 49). With obesity rates rising, extrapolation of these data predicts higher rates of cancer in the future, particularly among individuals who are overweight or obese. Cancer treatment has undergone a revolution over the last decade and we have now entered the era of immunotherapy, but obesity is associated with dysfunction of several immune cells important for killing tumors including dendritic cells, T cells, NK cells, and macrophages (4, 50–52). These observations raise critical questions about the efficacy of cancer immunotherapy in overweight and obese patients, leading to the hypothesis that body mass may be prognostic for patient outcomes after treatment with immunotherapy.

Testing this hypothesis has led to a flurry of clinical reports but achieving consensus has been challenging. Some studies have correlated obesity with poor outcomes (5–7), wheras others have observed either no effect or concluded that obesity actually benefits some patients with cancer receiving immunotherapy, and that sex differences may influence this benefit (8, 9). One proposed mechanism for improved responses to PD1 checkpoint blockade is that obesity-associated leptin directly induces PD1 expression on T cells, making them more amenable to blockade (9). But this was not borne out by our data or other clinical studies where patient survival was statistically

indistinguishable for obese and nonobese patients treated with PD1/L1-targeted checkpoint blockade (8, 53). In agreement with the McQuade and colleagues study (8), we did observe a slight survival advantage in male obese patients with melanoma treated with anti-CTLA4. However, our prospective analysis of 68 patients with cancer and 21 healthy donors showed no evidence that BMI or serum leptin correlated with PD-1 expression on T cells, suggesting that leptin-induced PD1 expression cannot explain this outcome. At this point, we are left with several clinical studies that reach different conclusions. When taken together, our interpretation is that BMI as a lone metric of obesity is not able to consistently predict cancer patient outcomes, and in those cases where BMI was associated with modest changes in survival, we still lack a unifying mechanistic explanation.

It is not clear why a correlation between leptin and PD1 was observed in one study but not in others. This discrepancy could stem from differences in the individuals that were examined. For example, in the study by Wang and colleagues (9), PD1 and leptin protein expression was only assessed in a group of 21 healthy female volunteers, whereas our analysis focused on a more diverse group of male and female patients with either melanoma, breast cancer, or lymphoma, as well as male and female healthy volunteers. It is also possible that variations in immune phenotype differed because of unknown influences associated with geography, lifestyle, diet, or metabolic health—independent of obesity. This is not to say that obesity and its complex array of comorbidities have no influence on tumor immunity or responses to checkpoint blockade immunotherapy, but obese patients are quite diverse. We predict that factors related to environment, metabolism, lipidomics, and microbiome are more likely to be the real drivers of heterogeneity in immune function among patients, regardless of BMI. Factors such as these are not reflected in BMI and can range in both prominence and severity among patients with a spectrum of body masses. Thus, a BMI over 30 is neither required nor sufficient to experience these "obesity-associated" comorbidities that have the potential to influence immunotherapy outcomes.

To gain mechanistic insight into why some patients respond better than others to immunotherapy, independent of BMI, we compared plasma lipid species among patients with melanoma and breast cancer. Using a multiparameter composite immune score, we correlated higher levels of total cholesterol, LDL, and ox-LDL with reduced $CD8^+$ T-cell effector function. In support of this, we observed a direct inhibitory effect of ox-LDL on human $CD8^+$ T-cell responses after *in vitro* stimulation, suggesting that cholesterol, LDL, and ox-LDL have the potential impair responses to immunotherapy. Indeed, in a limited cohort of patients with cancer treated with anti-PD1/L1 immunotherapy, we correlated higher concentrations of plasma LDL with reduced OS.

In addition to having an impact on immunity, oxidized lipids can also bring about changes to tumor cells directly. We hypothesized that oxidative stress in the tumor microenvironment and the presence of oxidized lipids may fortify tumor cells by triggering protective mechanisms that insulate them from potential harm mediated by the immune system, thereby offering resistance to immunotherapy. HO-1 is a cytoprotective molecule induced under conditions of oxidative stress and in response to oxidized lipids (36). From a clinical perspective, HO-1 expression in melanoma tumors correlated with reduced patient survival and has previously been identified as a possible molecular target to improve existing cancer therapies (38, 46, 54). Our results confirmed that LDL, and in particular ox-LDL, induced HO-1 in both murine and human melanoma tumors, protecting these tumor cells from apoptosis. Furthermore, we established HO-1 expression as a mechanism of resistance to immunotherapy in mouse models of melanoma and breast cancer, where HO-1 could be targeted *in vivo* to improve anti-PD1 efficacy. Contrary to our initial prediction, inhibition of HO-1 did not alter antitumor immunity. Instead, our data suggest that inhibiting HO-1 interferes with a tumor cell–specific cytoprotective program, making tumor cells more susceptable to immune-mediated killing.

In conclusion, our study provides evidence that obesity, as defined by BMI, does not accurately predict patient outcomes following treatment with checkpoint blockade immunotherapy for cancer. Our results raise questions about the proposed mechanism linking increased PD1 expression to elevated leptin in obese individuals. Rather, our study of cancer patient immune cell function and corresponding lipid profiles provide insight into how oxidized lipids affect T-cell function while also driving a cellular stress response in mouse and human tumors. This response relied on increased expression of the cytoprotective enzyme HO-1, which endowed tumors with the ability to resist immune-mediated apoptosis. Our study also exposed HO-1 as a key vulnerability that may be exploited therapeutically to weaken tumor cells with some degree of specificity. Thus, HO-1 represents a promising molecular target for combination treatment strategies to improve the efficacy of cancer immunotherapy.

Authors' Disclosures

J. Kline reports grants from Merck during the conduct of the study, as well as personal fees from Kite/Gilead, Seattle Genetics, MorphoSys, Karyopharm, and iTeos outside the submitted work. No disclosures were reported by the authors.

Authors' Contributions

N. Khojandi: Conceptualization, data curation, formal analysis, investigation, methodology, writing–original draft, writing–review and editing. **L.M. Kuehm:** Data curation, formal analysis, investigation, methodology. **A. Piening:** Data curation, formal analysis, investigation, methodology. **M.J. Donlin:** Formal analysis, validation, investigation, methodology. **E.C. Hsueh:** Resources. **T.L. Schwartz:** Resources. **K. Farrell:** Resources. **J.M. Richart:** Resources. **E. Geerling:** Data curation, formal analysis, investigation, methodology. **A.K. Pinto:** Resources, supervision, validation, investigation, methodology. **S.L. George:** Resources, supervision, validation. **C.J. Albert:** Formal analysis, investigation, methodology. **D.A. Ford:** Supervision, validation, investigation, methodology. **X. Chen:** Data curation, formal analysis, investigation, methodology. **J. Kline:** Resources, supervision, validation, investigation, methodology. **R.M. Teague:** Conceptualization, resources, data curation, formal analysis, supervision, funding acquisition, validation, investigation, methodology, writing–original draft, project administration, writing–review and editing.

Acknowledgments

The authors thank Sherri Koehm and Joy Eslick for technical assistance with flow cytometry, and Sandra Miller and Stephanie Brem for assistance in obtaining patient samples. They also thank Ben Heckert, Debra King, and April Stephens for assistance with retrospective patient data from the SLU Cancer Center.

Research reported in this article was supported by grants from the NIH (S10OD025246) to D.A. Ford, the Alvin J. Siteman Comprehensive Cancer Center (P30 CA091842) and from the NIH NCI (R01 CA238705) to R.M. Teague.

The costs of publication of this article were defrayed in part by the payment of page charges. This article must therefore be hereby marked *advertisement* in accordance with 18 U.S.C. Section 1734 solely to indicate this fact.

Received April 29, 2020; revised October 7, 2020; accepted December 3, 2020; published first December 10, 2020.

References

1. Wolchok JD, Chiarion-Sileni V, Gonzalez R, Rutkowski P, Grob JJ, Cowey CL, et al. Overall survival with combined nivolumab and ipilimumab in advanced melanoma. N Engl J Med 2017;377:1345–56.
2. Eroglu Z, Zaretsky JM, Hu-Lieskovan S, Kim DW, Algazi A, Johnson DB, et al. High response rate to PD-1 blockade in desmoplastic melanomas. Nature 2018; 553:347–50.
3. Klevorn LE, Teague RM. Adapting cancer immunotherapy models for the real world. Trends Immunol 2016;37:354–63.
4. Kanneganti TD, Dixit VD. Immunological complications of obesity. Nat Immunol 2012;13:707–12.
5. Incio J, Ligibel JA, McManus DT, Suboj P, Jung K, Kawaguchi K, et al. Obesity promotes resistance to anti-VEGF therapy in breast cancer by up-regulating IL-6 and potentially FGF-2. Sci Transl Med 2018;10:eaag0945.
6. Ferro M, Vartolomei MD, Russo GI, Cantiello F, Farhan ARA, Terracciano D, et al. An increased body mass index is associated with a worse prognosis in patients administered BCG immunotherapy for T1 bladder cancer. World J Urol 2019;37:507–14.
7. Fang S, Wang Y, Dang Y, Gagel A, Ross MI, Gershenwald JE, et al. Association between body mass index, C-reactive protein levels, and melanoma patient outcomes. J Invest Dermatol 2017;137:1792–5.
8. McQuade JL, Daniel CR, Hess KR, Mak C, Wang DY, Rai RR, et al. Association of body-mass index and outcomes in patients with metastatic melanoma treated with targeted therapy, immunotherapy, or chemotherapy: a retrospective, multicohort analysis. Lancet Oncol 2018;19:310–22.
9. Wang Z, Aguilar EG, Luna JI, Dunai C, Khuat LT, Le CT, et al. Paradoxical effects of obesity on T cell function during tumor progression and PD-1 checkpoint blockade. Nat Med 2019;25:141–51.
10. Murphy KA, James BR, Sjaastad FV, Kucaba TA, Kim H, Brincks EL, et al. Cutting edge: elevated leptin during diet-induced obesity reduces the efficacy of tumor immunotherapy. J Immunol 2018;201:1837–41.
11. Tomiyama AJ, Hunger JM, Nguyen-Cuu J, Wells C. Misclassification of cardiometabolic health when using body mass index categories in NHANES 2005–2012. Int J Obes 2016;40:883–6.
12. Banack HR, Stokes A. The 'obesity paradox' may not be a paradox at all. Int J Obes 2017;41:1162–3.
13. Delimaris I, Faviou E, Antonakos G, Stathopoulou E, Zachari A, Dionyssiou-Asteriou A. Oxidized LDL, serum oxidizability and serum lipid levels in patients with breast or ovarian cancer. Clin Biochem 2007;40:1129–34.
14. Bradley AS, Ford B, Bansal AS. Altered functional B cell subset populations in patients with chronic fatigue syndrome compared to healthy controls. Clin Exp Immunol 2013;172:73–80.
15. Han X, Gross RW. Shotgun lipidomics: electrospray ionization mass spectrometric analysis and quantitation of cellular lipidomes directly from crude extracts of biological samples. Mass Spectrom Rev 2005;24:367–412.
16. Bowden JA, Shao F, Albert CJ, Lally JW, Brown RJ, Procknow JD, et al. Electrospray ionization tandem mass spectrometry of sodiated adducts of cholesteryl esters. Lipids 2011;46:1169–79.
17. Hodi FS, O'Day SJ, McDermott DF, Weber RW, Sosman JA, Haanen JB, et al. Improved survival with ipilimumab in patients with metastatic melanoma. N Engl J Med 2010;363:711–23.
18. Considine RV, Sinha MK, Heiman ML, Kriauciunas A, Stephens TW, Nyce MR, et al. Serum immunoreactive-leptin concentrations in normal-weight and obese humans. N Engl J Med 1996;334:292–5.
19. Dayakar A, Chandrasekaran S, Veronica J, Bharadwaja V, Maurya R. Leptin regulates granzyme-A, PD-1 and CTLA-4 expression in T cell to control visceral leishmaniasis in BALB/c mice. Sci Rep 2017;7:14664.
20. Naylor C, Petri WA Jr. Leptin regulation of immune responses. Trends Mol Med 2016;22:88–98.
21. Saucillo DC, Gerriets VA, Sheng J, Rathmell JC, Maciver NJ. Leptin metabolically licenses T cells for activation to link nutrition and immunity. J Immunol 2014; 192:136–44.
22. Lord GM, Matarese G, Howard JK, Baker RJ, Bloom SR, Lechler RI. Leptin modulates the T-cell immune response and reverses starvation-induced immunosuppression. Nature 1998;394:897–901.
23. Kuehm LM, Khojandi N, Piening A, Klevorn LE, Geraud SC, McLaughlin NR, et al. Fructose promotes cytoprotection in melanoma tumors and resistance to immunotherapy. Cancer Immunol Res 2021;9:227–38.
24. Rivadeneira DB, DePeaux K, Wang Y, Kulkarni A, Tabib T, Menk AV, et al. Oncolytic viruses engineered to enforce leptin expression reprogram tumor-infiltrating T cell metabolism and promote tumor clearance. Immunity 2019;51: 548–60.
25. Hansson GK, Hermansson A. The immune system in atherosclerosis. Nat Immunol 2011;12:204–12.
26. Quinn MT, Parthasarathy S, Fong LG, Steinberg D. Oxidatively modified low density lipoproteins: a potential role in recruitment and retention of monocyte/macrophages during atherogenesis. Proc Natl Acad Sci U S A 1987;84:2995–8.
27. Steinberg D, Parthasarathy S, Carew TE, Khoo JC, Witztum JL. Beyond cholesterol. Modifications of low-density lipoprotein that increase its atherogenicity. N Engl J Med 1989;320:915–24.
28. Hermansson A, Ketelhuth DF, Strodthoff D, Wurm M, Hansson EM, Nicoletti A, et al. Inhibition of T cell response to native low-density lipoprotein reduces atherosclerosis. J Exp Med 2010;207:1081–93.
29. Ma X, Bi E, Lu Y, Su P, Huang C, Liu L, et al. Cholesterol induces CD8(+) T cell exhaustion in the tumor microenvironment. Cell Metab 2019;30:143–56.
30. Parthasarathy S, Raghavamenon A, Garelnabi MO, Santanam N. Oxidized low-density lipoprotein. Methods Mol Biol 2010;610:403–17.
31. Kuzu OF, Noory MA, Robertson GP. The role of cholesterol in cancer. Cancer Res 2016;76:2063–70.
32. Nielsen SF, Nordestgaard BG, Bojesen SE. Statin use and reduced cancer-related mortality. N Engl J Med 2012;367:1792–802.
33. Yang W, Bai Y, Xiong Y, Zhang J, Chen S, Zheng X, et al. Potentiating the antitumour response of CD8(+) T cells by modulating cholesterol metabolism. Nature 2016;531:651–5.
34. Lu J, Mitra S, Wang X, Khaidakov M, Mehta JL. Oxidative stress and lectin-like ox-LDL-receptor LOX-1 in atherogenesis and tumorigenesis. Antioxid Redox Signal 2011;15:2301–33.
35. Balzan S, Lubrano V. LOX-1 receptor: a potential link in atherosclerosis and cancer. Life Sci 2018;198:79–86.
36. Ishikawa K, Navab M, Leitinger N, Fogelman AM, Lusis AJ. Induction of heme oxygenase-1 inhibits the monocyte transmigration induced by mildly oxidized LDL. J Clin Invest 1997;100:1209–16.
37. Stocker R, Perrella MA. Heme oxygenase-1: a novel drug target for atherosclerotic diseases? Circulation 2006;114:2178–89.
38. Alaoui-Jamali MA, Bismar TA, Gupta A, Szarek WA, Su J, Song W, et al. A novel experimental heme oxygenase-1-targeted therapy for hormone-refractory prostate cancer. Cancer Res 2009;69:8017–24.
39. Di Biase S, Lee C, Brandhorst S, Manes B, Buono R, Cheng CW, et al. Fasting-mimicking diet reduces HO-1 to promote T cell-mediated tumor cytotoxicity. Cancer Cell 2016;30:136–46.
40. Banerjee P, Basu A, Wegiel B, Otterbein LE, Mizumura K, Gasser M, et al. Heme oxygenase-1 promotes survival of renal cancer cells through modulation of apoptosis- and autophagy-regulating molecules. J Biol Chem 2012; 287:32113–23.
41. Lin Q, Weis S, Yang G, Weng YH, Helston R, Rish K, et al. Heme oxygenase-1 protein localizes to the nucleus and activates transcription factors important in oxidative stress. J Biol Chem 2007;282:20621–33.
42. Was H, Cichon T, Smolarczyk R, Rudnicka D, Stopa M, Chevalier C, et al. Overexpression of heme oxygenase-1 in murine melanoma: increased proliferation and viability of tumor cells, decreased survival of mice. Am J Pathol 2006; 169:2181–98.
43. Curran MA, Montalvo W, Yagita H, Allison JP. PD-1 and CTLA-4 combination blockade expands infiltrating T cells and reduces regulatory T and myeloid cells within B16 melanoma tumors. Proc Natl Acad Sci U S A 2010; 107:4275–80.
44. Kuehm LM, Wolf K, Zahour J, DiPaolo RJ, Teague RM. Checkpoint blockade immunotherapy enhances the frequency and effector function of murine tumor-infiltrating T cells but does not alter TCRbeta diversity. Cancer Immunol Immunother 2019;68:1095–106.
45. Gozzelino R, Jeney V, Soares MP. Mechanisms of cell protection by heme oxygenase-1. Annu Rev Pharmacol Toxicol 2010;50:323–54.
46. Berberat PO, Dambrauskas Z, Gulbinas A, Giese T, Giese N, Kunzli B, et al. Inhibition of heme oxygenase-1 increases responsiveness of pancreatic cancer cells to anticancer treatment. Clin Cancer Res 2005;11:3790–8.
47. Renehan AG, Tyson M, Egger M, Heller RF, Zwahlen M. Body-mass index and incidence of cancer: a systematic review and meta-analysis of prospective observational studies. Lancet 2008;371:569–78.
48. Lauby-Secretan B, Scoccianti C, Loomis D, Grosse Y, Bianchini F, Straif K, et al. Body fatness and cancer–viewpoint of the IARC working group. N Engl J Med 2016;375:794–8.

49. Sergentanis TN, Antoniadis AG, Gogas HJ, Antonopoulos CN, Adami HO, Ekbom A, et al. Obesity and risk of malignant melanoma: a meta-analysis of cohort and case-control studies. Eur J Cancer 2013;49:642–57.
50. Aguilar EG, Murphy WJ. Obesity induced T cell dysfunction and implications for cancer immunotherapy. Curr Opin Immunol 2018;51:181–6.
51. James BR, Tomanek-Chalkley A, Askeland EJ, Kucaba T, Griffith TS, Norian LA. Diet-induced obesity alters dendritic cell function in the presence and absence of tumor growth. J Immunol 2012;189:1311–21.
52. Michelet X, Dyck L, Hogan A, Loftus RM, Duquette D, Wei K, et al. Metabolic reprogramming of natural killer cells in obesity limits antitumor responses. Nat Immunol 2018;19:1330–40.
53. Donnelly D, Bajaj S, Yu J, Hsu M, Balar A, Pavlick A, et al. The complex relationship between body mass index and response to immune checkpoint inhibition in metastatic melanoma patients. J Immunother Cancer 2019;7:222.
54. Podkalicka P, Mucha O, Jozkowicz A, Dulak J, Loboda A. Heme oxygenase inhibition in cancers: possible tools and targets. Contemp Oncol 2018;22:23–32.